Astronomy & Astrophysics manuscript no. main
August 31, 2016

Lab 3

Radio Interferometry at X Band

Ramsey Karim
with R. Bentley and S. Wishnek

University of California, Berkeley
HAIL SAGAN Research Group

August 31, 2016

ABSTRACT

The Orion Nebula and the Sun were observed horizon-to-horizon at 10.1 GHz with the single-baseline ($B \approx 16\ m$) interferometer on top of New Campbell Hall. The Orion data were compared to predictions and then used to fit the North-South and East-West baseline projections using a brute-force least squares method. The data show $B_{ew} = 15.08 \pm 8.2 \cdot 10^{-5}\ m$ and $B_{ns} = 1.601 \pm 1.0 \cdot 10^{-4}\ m$. The Sun data were compared to a predicted amplitude modulation pattern in order to estimate the angular diameter of the Sun, which the data show is 0.57°.

1. Introduction

Radio astronomy often involves more than one antenna. Of course, one antenna works; the last lab report walked through several observations with the Horn, a single antenna on the roof of Campbell, and the observations resulted in meaningful data. However, most single-antenna telescopes with circular dishes are limited in angular resolution simply as $\theta = 1.22 \times \lambda/D$, where θ is angular resolution, 1.22 has to do with the circular shape of the dish, λ is the wavelength of the observation, and D is the diameter of the collecting dish.

Here arises an obvious dilemma: an astronomer can sacrifice angular resolution with a small, easy-to-build dish, or s/he can spend a lot of money to make a large dish with better angular resolution. A large dish may be well worth the money for a major observatory or an important project; the Arecibo Observatory in Puerto Rico boasts the largest single-aperture telescope in the world, at an impressive diameter of 305 meters[1], while the Green Bank Observatory in West Virginia has claim to the largest fully steerable telescope[2] with a diameter of 100 meters. Both of these telescopes have quite decent angular resolution; at 21 cm, for example, the Green Bank telescope has a resolution of about 9 arcminutes, while the Arecibo telescope has a hefty 3.5 arcminutes. Yet there exists a telescope with a minimum 21 cm angular resolution of 5 milliarcseconds — 42 times better than that of Arecibo. How did astronomers achieve such great resolution? Interferometers.

The 5 milliarcsecond resolution telescope is the Very Long Baseline Array (VLBA). It is an array of 10 radio telescopes spread out across North America, from Hawaii to the Virgin Islands, and since interferometer angular resolution is approximately $R = \lambda/B$, where R is the resolution and B is the baseline, the massive baseline distance of the VLBA gives it good resolution. What are interferometers and what makes them special?

[1] 1000 feet sounds even *more* impressive!
[2] And in fact the largest steerable ground-based object in the world

1.1. Basic Interferometry

Interferometers are sets of two or more telescopes that mix their measured signals together in order to compare phases. This suggests that the individual antennas aren't as important as the relationships *between* each one; objectively, each pair of antennas only has one distinct quality: distance, which is called baseline in radio interferometry.

The simplest interferometer[3] is the two-element array, since it has just one baseline. The two antennas track the same object across the sky[4] and send their signals to a mixer;[5] the sum frequency is filtered out so only the difference remains. As the object moves across the sky, each measured voltage from the mixed and filtered signal is associated with the object's position on the sky, most notably its hour angle. The object's declination and the observatory's terrestrial latitude also come into play, but the main independent variable is the hour angle of the source.[6] The resulting signal is essentially a diffraction pattern across the sky[7]; this pattern is called the fringe.

1.1.1. The Fringe

The fringe pattern of an object, as previously mentioned, depends on the observer's terrestrial latitude and the object's declination and hour angle,[8] assuming a point source.

In order to derive the fringe pattern, a good astronomer should start from the beginning: the incoming signal. The incoming signal comes from a single source and is measured by two antennas. The distance to each antenna determines at what phase the signal will be measured by that antenna; when the sig-

[3] As every radio astronomy lesson begins
[4] More generally, they observe the same area of the sky, but we won't get into immobile antennas in this lab.
[5] Which we already covered in the last lab
[6] Hour angle will be mentioned quite frequently, and always refers to the hour angle of the *source*, unless otherwise specified
[7] As if baseline were an aperture, as in classical diffraction
[8] It also depends on the diameter of the source if it is not a point source

nals are mixed, the phase difference[9] is measured. The phase difference depends on the pathlength difference between the two antennas, which is the difference in distance traveled by light from the same source to different destinations. The phase difference will cycle constantly as the pathlength difference changes, and so the mixed and filtered signal will oscillate. This is the fringe.

Mathematically, the two signals received by the antennas are

$$E_1(t) = \cos(2\pi\nu t) \tag{1}$$

and

$$E_2(t) = \cos(2\pi\nu[t + \tau_{tot}]) \tag{2}$$

where ν is the signal frequency and $\tau_{tot} = \tau_g(ha) + \tau_c$ is the total delay, which includes both pathlength difference as a function of hour angle $\tau_g(ha)$ and any cable delay τ_c between the two antennas. The signals are multiplied together, and after the sum frequency is filtered out, the difference remains:

$$F(ha) = \cos(2\pi\nu[\tau_{tot}]) = \cos(2\pi\nu[\tau_g(ha) + \tau_c]) \tag{3}$$

Stepping through another trigonometry identity:

$$F(ha) = \cos(2\pi\nu\tau_c)\cos(2\pi\nu\tau_g(ha)) - \sin(2\pi\nu\tau_c)\sin(2\pi\nu\tau_g(ha)) \tag{4}$$

Now take a look at Equation 4; it depends on τ_c, but no one wants to bother measuring the cable delays. For the purpose of this lab, they're not important and they can be hand-waved away into constants:

$$F(ha) = A\cos(2\pi\nu\tau_g(ha)) + B\sin(2\pi\nu\tau_g(ha)) \tag{5}$$

It is evident that this is a function of hour angle, but the hour angle term is nested inside trig functions. The expression for $\nu\tau_g(ha)$ will not be derived here; it includes baseline (east-west and north-south are kept separate), wavelength, declination, and the observer's terrestrial latitude:

$$\nu\tau_g(ha) = \left[\frac{B_{ew}}{\lambda}\cos(\delta)\right]\sin(ha) + \left[\frac{B_{ns}}{\lambda}\sin(L)\cos(\delta)\right]\cos(ha) \tag{6}$$

Substituting Equation 6 into Equation 5 yields the fringe frequency, which can be fitted to data to solve for A and B, but which requires knowledge of declination δ and the baselines B_{ew} and B_{ns}. This fit will be done in the Analysis section. It is assumed that the astronomer is well aware of his or her terrestrial latitude and the frequency at which s/he is observing.

1.1.2. Local Fringe Frequency

It is worth briefly mentioning the concept of the local fringe frequency, which is the frequency at which the fringe is currently oscillating, given a small slice of hour angle Δha. Given a Taylor expansion of $\sin(ha)$ or $\cos(ha)$ around the current hour angle of the source, one derives the local fringe frequency as a function of hour angle:

$$f_f(ha) = \left[\frac{B_{ew}}{\lambda}\cos(\delta)\right]\cos(ha) - \left[\frac{B_{ns}}{\lambda}\sin(L)\cos(\delta)\right]\sin(ha) \tag{7}$$

The complete fringe pattern varies in local frequency, as one can see in the two right-hand subplots of Figure 1. A plot of the local fringe frequency gives the predicted progression of this local frequency, as seen in Figure 2.

[9] Absolute phase is meaningless; the phase difference is what matters

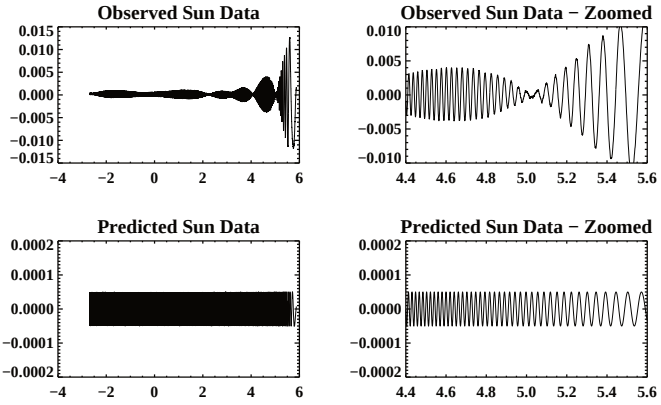

Fig. 1. Theoretical fringe and measured fringe plotted against hour angle. Notice that the theoretical plot lacks the modulation of the observation; this is addressed in a later part of the lab. For now, just note that the local frequencies seem to match up at the same hour angles.

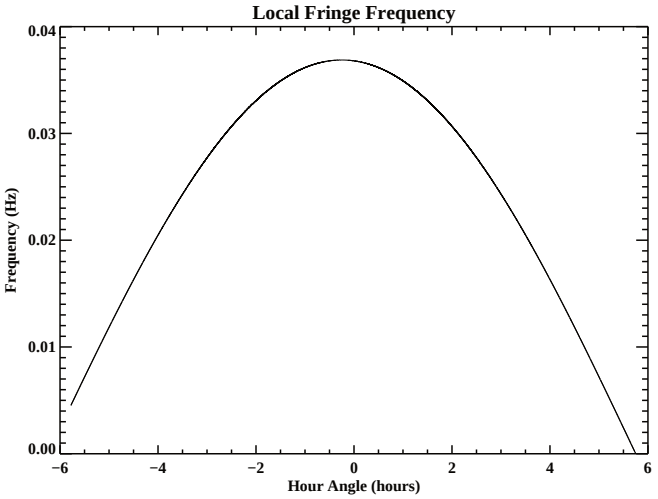

Fig. 2. Local fringe frequency plotted against source hour angle. Note that Orion and the spring Sun both have a declination of $0° \pm 5°$, so both can be modeled approximately by the same local fringe frequency prediction plot.

1.1.3. Extended Sources

While many sources can be approximated as point sources, objects like the Sun and the Moon cannot; they have a nontrivial angular width. Every part of these sources contributes to the fringe as an infinitesimal 'point source', and so every so often, the fringes will collectively interfere and yield a global zero in the entire fringe. This sort of behavior creates a modulation in the fringe pattern; the Sun's modulation is obvious, as seen in the top two subplots in Figure 1. The modulation depends on the local fringe frequency and the radius of the object, so if the local fringe frequency can be determined as a function of hour angle, as in Equation 7, then the modulation function is a simple calculation away. This will be discussed more later, during the Analysis section of the report.

2. Observations

This lab involves two main sets of data, both recorded using the interferometer on the roof of New Campbell Hall at 10.1 GHz,[10] one of the Orion Nebula and one of the Sun.[11]

2.1. The New Campbell Hall Interferometer

The interferometer on the roof of NCH consists of two antennas, two local oscillators corresponding to two mixing stages, and a series of amplifiers and such, as shown in Figure 3. The signal is measured by both antennas and mixed with a local oscillator frequency ν_{LO} corresponding to the desired observation frequency ν as $\nu_{LO} = \nu - 1.7\ GHz$. The Hail Sagan Research Group sought to observe at 10.1 GHz for this project and so the local oscillator was set at 8.4 GHz for all measurements. Each ~1.7 GHz signal is fed into an isolator that prevents reflections and then two 20dB amplifiers, then mixed with a 1370 MHz local oscillator that takes the signals down to about 330 MHz. The signals are passed through 30 MHz wide bandpass filters centered around 327 MHz, amplified a lot more, and finally mixed together and passed through a low-pass RC filter with a time constant of ~1 second. The signal is then digitally sampled. The RC filter gives the entire process a sample rate of just about 1 Hz.

The resulting data are received by the `STARTCHART1` procedure in volts. The procedure records LST, Julian day, and voltage for every measurement, and also right ascension and declination if the `SUN` or `MOON` keywords are used. The interferometer is pointed at the source using the `FOLLOW` procedure, which takes arguments of right ascension and declination and saves the tracking information in a file. The `FOLLOW` and `STARTCHART1` procedures operate independently, so a pointing error on the part of `FOLLOW` will not interrupt the measurement of `STARTCHART1`. The final Orion Nebula and Sun observations were taken horizon-to-horizon. Orion was taken on Julian Day 2457453.4-8, which was 2 P.M., March 5th, 2016, to just after midnight, March 6th. The Sun was taken for the last time on Julian Day 2457480.1-6, which was 7 A.M., April 1st, 2016, to 7:30 P.M. the same day.

2.2. The Orion Nebula

The position of the Orion Nebula was provided to the research group by their parent organization[12] as

$$r.a._{2000} = 05^h35^m17.3s \qquad dec_{2000} = -05°23'28" \tag{8}$$

which was converted to epoch-2016 coordinates using the `PRECESS` procedure

$$r.a._{2016} = 05^h36^m04.5s \qquad dec_{2016} = -05°22'54" \tag{9}$$

The resulting data are plotted in Figure 4 with their power spectrum. A filtered version of the set and its power spectrum are also shown. Notice that the local fringe frequencies in the noticeable sidebands are very similar to the predictions in Figure 2 of variation of frequency about 0.3 Hz. In the Analysis section, a least squares fit of the baseline to the data will be discussed.

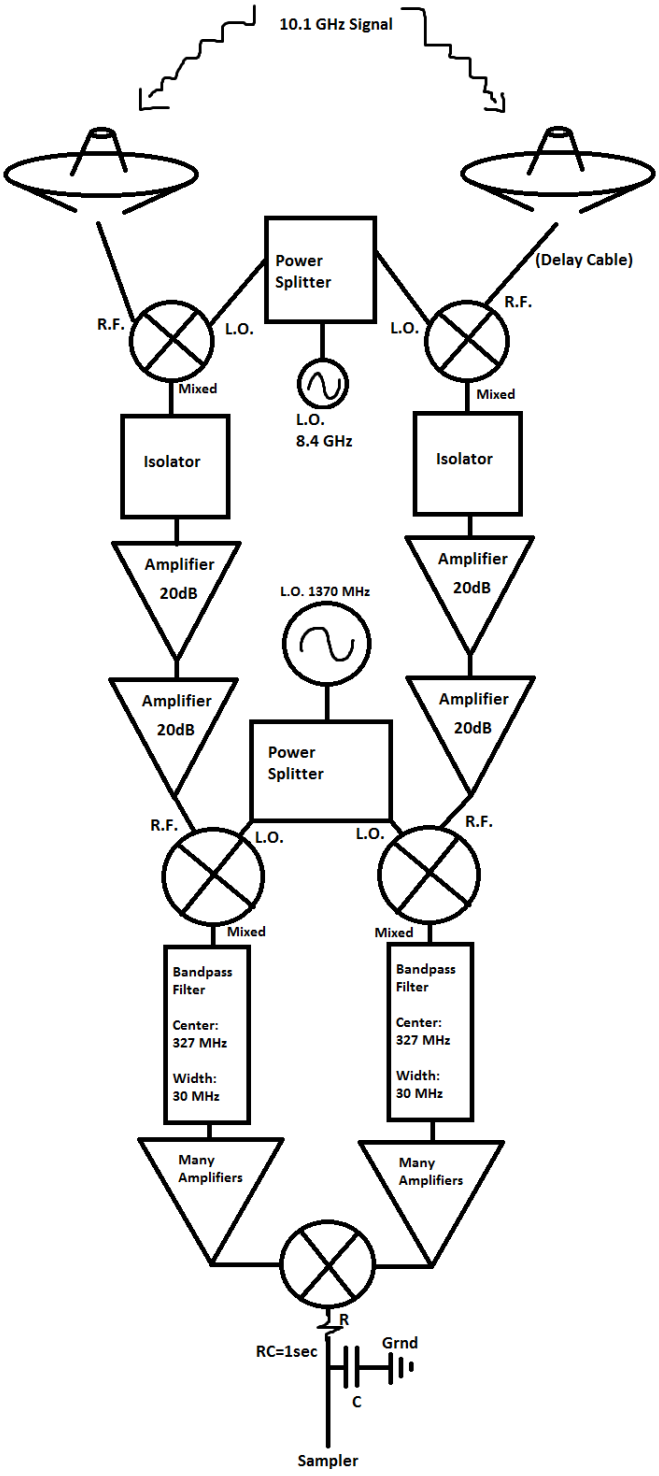

Fig. 3. Block diagram of the hardware between the interferometer and the sampler

2.3. The Sun

The position of the Sun can be found using the IDL procedure `ISUN`, and the `SUN` keyword in both `FOLLOW` and `STARTCHART1` tells each procedure to record and use the Sun's right ascension and declination in real time during the observation.[13] The Sun

[10] All measurements made in this lab were at 10.1 GHz; it will no longer be explicitly stated

[11] Several data sets were actually taken, but just one horizon-to-horizon set was used for the main calculations

[12] Known only by the name "Astronomy 121"

[13] The MOON keyword works the same way in both procedures

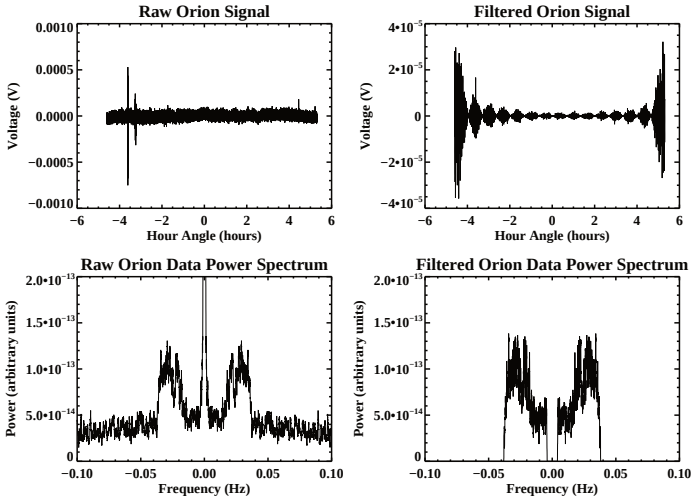

Fig. 4. Orion signal, power spectrum, and filtered signal and power spectrum.

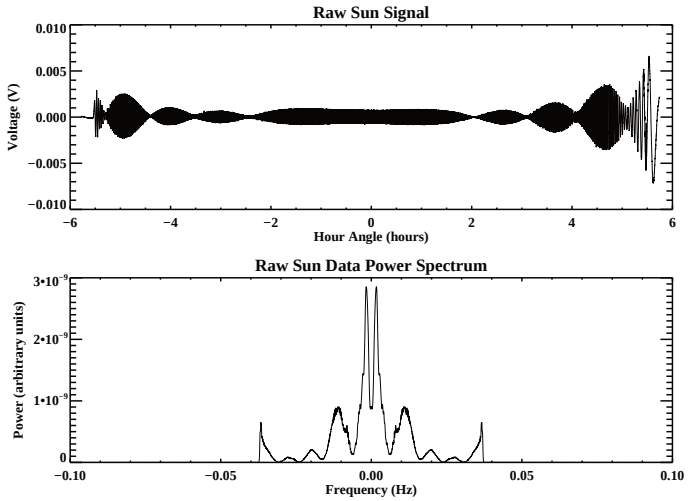

Fig. 5. Sun signal and power spectrum. The data are clear enough without filtering.

data were much clearer altogether than Orion, as seen in Figure 5.

These were the only two true measurements in this project; the rest was analysis using the collected data and will be discussed in the corresponding[14] Analysis section.

3. Analysis

Two observations were made: one of the Orion Nebula and one of the Sun. Both were taken horizon-to-horizon, so both contain about $12\,hr * \frac{60\,min}{1\,hr} * \frac{60\,sec}{1\,min} = 43000$ data.[15] Each set was analyzed differently. The basic processing was the same; the signal was examined, ends were trimmed, power spectrum examined, and signal filtered if deemed necessary. Beyond that, the Orion data and the Sun data had different purposes. The Orion data were used to find a baseline estimate given the known declination of the object, while the Sun data were used to find an estimate of the diameter of the Sun.

3.1. A Brief Word about the Moon

It would be prudent to mention at this point that the Moon was also observed during this project. While it would have been very nice to have Moon data to process in order to estimate the Moon's diameter as well, the research group experienced some difficulty obtaining the data. An observation was run on the Moon on April 2nd, 2016, from 4 A.M. to about 1 P.M. when it experienced premature termination by a third party, who reportedly told the group that it was consistently recording 0 volts. Upon examination of these suspect data, the group concluded that the data were in fact unusable for some unknown reason and was forced to abandon that effort.

3.2. Orion Analysis: Fit of Baseline to Data

The Orion data were used to find an estimate of the baseline of the interferometer pair. Recall Equations 5 and 6 from Section 1.1.1, recreated below as Equations 10 and 11.

$$F(ha) = A\cos(2\pi\nu\tau_g(ha)) + B\sin(2\pi\nu\tau_g(ha)) \tag{10}$$

$$\nu\tau_g(ha) = \left[\frac{B_{ew}}{\lambda}\cos(\delta)\right]\sin(ha) + \left[\frac{B_{ns}}{\lambda}\sin(L)\cos(\delta)\right]\cos(ha) \tag{11}$$

The baseline is split into North-South and East-West projections and buried in $\nu\tau_g$. The fringe has a nonlinear dependence on the baselines since they are inside trig functions, so linear least squares is not (yet) an option.

3.2.1. Brute Force Least Squares Fit of the Baseline

But there is still hope. Rewrite Equation 11 with the substitutions

$$Q_{ew} = \left[\frac{B_{ew}}{\lambda}\cos(\delta)\right]$$

and

$$Q_{ns} = \left[\frac{B_{ns}}{\lambda}\sin(L)\cos(\delta)\right]$$

Now Q_{ew} and Q_{ns} will serve as variables containing both baselines and declination in order to simplify the expression and allow for possible fit of either variable given knowledge of the other. This yields the equation:

$$\nu\tau_g(ha) = Q_{ew}\sin(ha) + Q_{ns}\cos(ha) \tag{12}$$

Plugging Equation 12 into Equation 10 yields the fringe pattern. Of course, one needs values for Q_{ew} and Q_{ns}, and then the problem becomes linear once again, since the only coefficients left to fit are A and B to the linear combination of $\cos(2\pi\nu\tau_g(ha))$ and $\sin(2\pi\nu\tau_g(ha))$, respectively. A and B aren't important, really; the wellness of their fit is of much more interest. Remember that the objective is to fit the Qs to the data. It is conceivable, then, to populate an array indexed by guesses of Q_{ew} and Q_{ns} with the sums of residual squares from the fits of A and B corresponding to each Q guess combination. That was a bit of a mouthful; it would be prudent to include a visual aide.

[14] And aptly named

[15] This is a proper use of the word data because "data" is the plural form of "datum." In fact, this particular report only ever uses the word "data" correctly.

Imagine an array of m by n elements, indexed effectively by n guesses for Q_{ew} and m guesses for Q_{ns}:

$$\mathbf{Guesses} = \begin{bmatrix} q_{ew,1}, q_{ns,1} & \cdots & q_{ew,n}, q_{ns,1} \\ \vdots & q_{ew,i}, q_{ns,j} & \vdots \\ q_{ew,1}, q_{ns,m} & \cdots & q_{ew,n}, q_{ns,m} \end{bmatrix}$$

Note that these aren't the array's values; they're just guesses of the Qs associated with each element. Then, for each element i, j, plug each guess combination into Equation 12 to get $\nu\tau_{g,ij}$. Create an $l \times 2$ array $\mathbf{X}$, where l is the number of data, using the two variables from Equation 10 evaluated at every hour angle (there are l total hour angles in the data set):

$$\mathbf{X} = \begin{bmatrix} \cos(2\pi\nu\tau_{g,ij}(ha_0)) & \sin(2\pi\nu\tau_{g,ij}(ha_0)) \\ \cos(2\pi\nu\tau_{g,ij}(ha_1)) & \sin(2\pi\nu\tau_{g,ij}(ha_1)) \\ \cos(2\pi\nu\tau_{g,ij}(ha_2)) & \sin(2\pi\nu\tau_{g,ij}(ha_2)) \\ \vdots & \vdots \\ \cos(2\pi\nu\tau_{g,ij}(ha_{l-1})) & \sin(2\pi\nu\tau_{g,ij}(ha_{l-1})) \end{bmatrix} \quad (13)$$

Now, this sets the data up for least squares fitting of the coefficients A and B, which can be said to reside in a vector $\beth$:

$$\mathbf{a} = \begin{bmatrix} A \\ B \end{bmatrix}$$

Let the observed data reside in a column vector $\mathbf{Y}$ of l elements. The vector $\mathbf{Y}$ can be written

$$\mathbf{Y} = \mathbf{X} \cdot \mathbf{a}$$

Now front multiply both sides by $\mathbf{X^T}$:

$$\mathbf{X^T} \cdot \mathbf{Y} = \mathbf{X^T} \cdot \mathbf{X} \cdot \mathbf{a}$$

The $\mathbf{X}and\mathbf{X^T}$ vectors are now neatly tucked away in a 2×2 matrix, which can safely be nullified on the right side of the equation by front multiplication of its inverse:

$$(\mathbf{X^T} \cdot \mathbf{X})^{-1} \cdot \mathbf{X^T} \cdot \mathbf{Y} = (\mathbf{X^T} \cdot \mathbf{X})^{-1} \cdot (\mathbf{X^T} \cdot \mathbf{X}) \cdot \mathbf{a}$$

$$(\mathbf{X^T} \cdot \mathbf{X})^{-1} \cdot \mathbf{X^T} \cdot \mathbf{Y} = \mathbf{I} \cdot \mathbf{a}$$

$$(\mathbf{X^T} \cdot \mathbf{X})^{-1} \cdot \mathbf{X^T} \cdot \mathbf{Y} = \mathbf{a}$$

The coefficient vector $\mathbf{a}$ has been isolated; it can be placed back into the relation $\mathbf{Y'} = \mathbf{X} \cdot \mathbf{a}$. The primed vector $\mathbf{Y'}$ is used in this expression to distinguish itself (the fit) from the observed data ($\mathbf{Y}$) since one cannot absolutely solve for all the *exact* data. $\mathbf{Y'}$ signifies that this is a fit to the data and not a perfect reproduction of them. Recall that the original plan was to populate that **Guesses** array with the corresponding sums of the residuals. In accordance with that plan, subtract $\mathbf{Y} - \mathbf{Y'}$ and then front multiply it by its transpose, effectively squaring each element and the summing across the entire vector:

$$(\mathbf{Y} - \mathbf{Y'})^{\mathbf{T}} - (\mathbf{Y} - \mathbf{Y'}) = RSS$$

Let RSS_{ij} represent the sum of the residual squares for that particular fit, and remember that each sum of residuals corresponds to a certain i, j combination. Now return to **Guesses** and assign the array element $\mathbf{Guesses}_{ij} = RSS_{ij}$. This results in an array of m by n elements, each corresponding to the minimum error of the A, B fit using the i^{th} guess for Q_{ew} and the j^{th} guess for Q_{ns}.

$$\mathbf{Guesses} = \begin{bmatrix} RSS_{11} & \cdots & RSS_{n1} \\ \vdots & RSS_{ij} & \vdots \\ RSS_{1m} & \cdots & RSS_{nm} \end{bmatrix}$$

The next step is to plot this using IDL's `COUNTOUR` procedure. The plot should center around a global minimum value of $RSS_{ij} = RSS_{IJ}$ where I, J are the indices of the best values for Q_{ew} and Q_{ns}.

Voilà! This is brute force least squares! Results will appear in the[16] Conclusion section.

3.3. Sun Analysis: Fit of Solar Angular Radius to Fringe Zeros

The Sun data set has a unique attribute that sets it apart from the Orion set: it has a significant amplitude modulation pattern, as one can see in Figure 5 from Section 2.3. Note that the Orion signal shown in Figure 4 appears in one of the plots to show similar modulation; this is not the case. That modulation is an artifact of the Fourier filtering. There could not be that much (if any at all) modulation in that signal, since it appears as a point source to an interferometer with low angular resolution.

The Sun, however, has enough of a visible angular diameter to act as multiple point sources whose fringes interfere, modulating the total fringe pattern and occasionally zeroing out the whole signal. The modulation function will not be derived here, but the computational form of the resulting integral will be shown below:

$$ModFn_{theory} = \frac{R}{N} \sum_{n=-N}^{n=+N} \left[1 - \left(\frac{n}{N}\right)^2\right]^{1/2} \cos\left(\frac{2\pi f_f n R}{N}\right) \quad (14)$$

Note that in Equation 14, R is the angular radius of the extended source, and the modulation depends nonlinearly on R, which eliminates any possibility of a simple linear least squares fit. A brute force least squares fit with a 1D array of guesses for R was attempted but resulted in a poorly fitted theoretical signal and an inaccurate R value. A better method for fitting R to the data turns out to be eyeballing the zeros of the modulating function compared to the zeros of the Sun signal; this eliminates error resulting from a 'least-squares-centric' approach, which doesn't explicitly take into account the zeros. This is as simple as coding Equation 14 (a clean iteration from -N to N, picking N on the order of tens to thousands) and manually changing the value of R. Figure 6 demonstrates the effect of changing R given some likely radius values.[17] Overplotting the modulation function onto the Sun signal makes the zeros easy to find and match via adjusting R.

4. Results

Now for the results. Each data set was processed and analyzed as explained in the previous Analysis section. The results of each analysis are as follows.

4.1. Orion Results

The goal of the Orion Nebula analysis was to fit the best possible values for Q_{ew} and Q_{ns} to the data using "brute force least squares." After running a long iteration with good Q resolution[18], the program settled upon the best Q values[19]:

$$Q_{ew} = 506.0 \pm 4.8 \cdot 10^{-4}$$

[16] Once again, aptly named

[17] We know that the angular diameter of the Sun is about half a degree

[18] Meaning the program iterated through many fractions of Qs

[19] The errors are derived from the diagonals of the covariance matrix, as in the Least Squares Lite publication

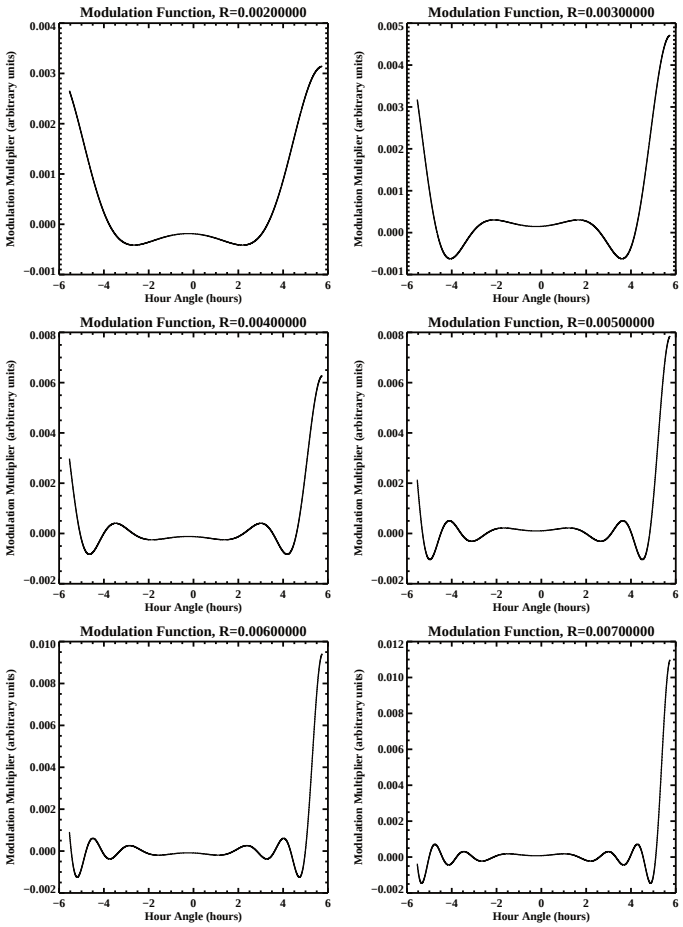

Fig. 6. Several modulation functions using different R values plotted against hour angle. Note that the number and location of zeros changes with every R.

$$Q_{ns} = 32.96 \pm 4.8 \cdot 10^{-4}$$

Given the Orion Nebula's declination, the latitude of New Campbell Hall, and the wavelength of a 10.1 GHz EM wave in a vacuum (2.968 cm), these both solve easily for the baselines:

$$B_{ew} = 15.08 \pm 8.2 \cdot 10^{-5}\ m$$

$$B_{ns} = 1.601 \pm 1.0 \cdot 10^{-4}\ m$$

These baseline values are very close to the actual total length of the baseline, which is about 16 meters, mostly East-West.

4.2. Sun Results

The goal of the Sun data analysis was to calculate the angular diameter of the Sun. The eyeballing method worked well for this purpose; the brute force least squares attempt gave zeros in the wrong places and suggested an angular radius of about 1.4°, which is a little too far off the known value of 2.5°. The eyeballing method worked much better, giving an angular radius of 0.005 *radians* or 0.29° and an angular diameter of

$$D = 0.57°$$

This is closer to the expected value of 0.5° and matches the prediction that the Sun looks larger in radio wavelengths due to the visibility of the corona. The least squares answer of Diameter = 2.8° fell below the visible wavelength angular diameter; it was both quite far from the known value and also on the wrong side of the predicted error. The value of Diameter = 0.57° looks a lot better; see Figure 9 for a side-by-side of the theoretical and measured fringes. They are surprisingly similar — choosing the right R value for the modulation function and multiplying it by a brute-force-least-squares fitted normalized[20] fringe pattern matches the observation data quite well. This suggests two pleasant conclusions: first, the theory used to predict the fringe is accurate, and second, the data are clean and the observation was successful.

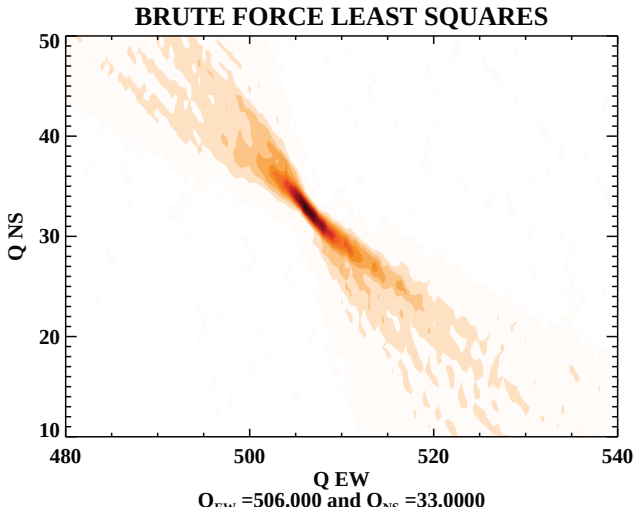

Fig. 7. A distant view of the successful brute force least squares iteration. The plot is indexed by Q guesses and contains values of sums of residual squares from the corresponding fit (exactly as the **Guesses** array worked). Note the obvious global minimum.

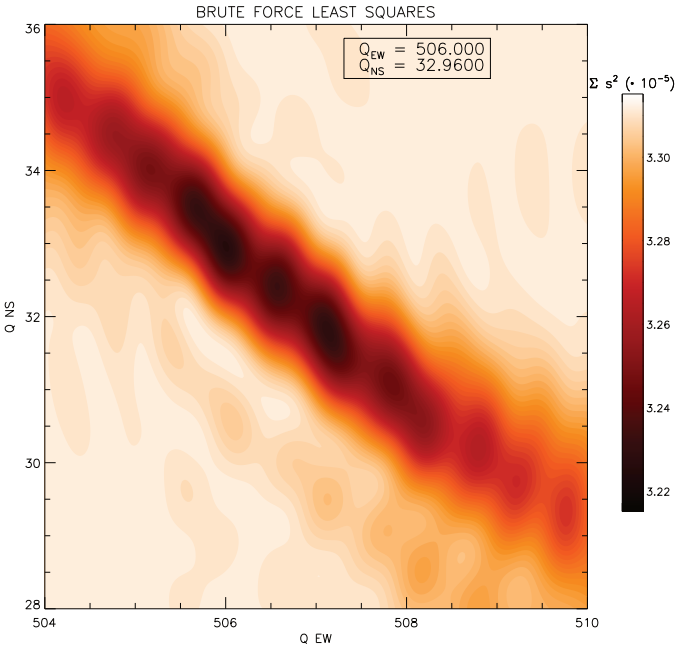

Fig. 8. A more zoomed-in view of the successful brute force least squares, yielding greater accuracy in visually locating the global minimum.

[20] Unmodulated

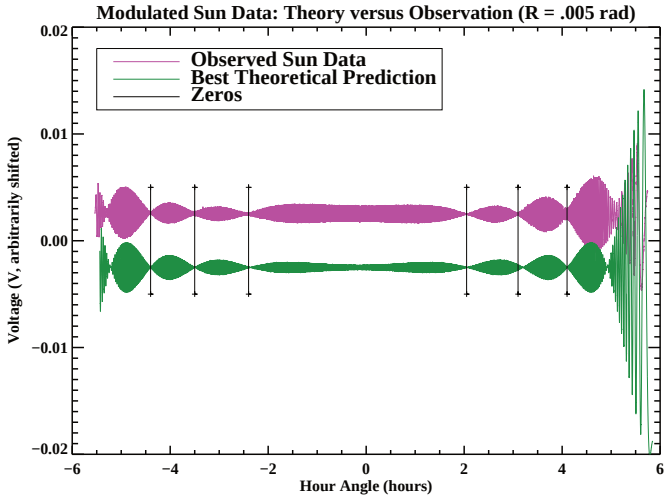

Fig. 9. Graph of observed and predicted modulated fringe patterns. The theoretical pattern is calculated with the best fit of $R = 0.005$ *radians*. Note that most of the zeros are lined up with great accuracy. The zeros at the end are not as well matched, but adjusting R any further in either direction had an adverse effect on the rest of the fit, so this was deemed the best.

5. Conclusion

This experiment was kept quite simple. It did not involve any of the angular resolution discussed in Section 1, nor did it involve any more than one baseline. What it did do was provide essential background and basic experience in using a *baseline* to observe a source. A single antenna yields a signal from the source, but a baseline yields a fringe pattern, which can be very useful.

Recall from the last lab that the Horn had to be pointed at the source in order for it to pick up the signal. This is all well and good if the position of the source is known. But what if it isn't? A single antenna would pick up less power from an off-center source without any other indication that the source is off center!

An interferometry array with a wide beam could pick up a signal from an off-center source, but the resulting fringe pattern contains information about the hour angle and the declination, given the baseline and the wavelength of observation. The research group fit the baselines to the data in this lab, but that was because of an unusual combination of confidence in the declination of the object and lack of confidence in the length and orientation of the baseline. Normally, the baseline is well known and the fit is the other way around; one can easily see from the equations in Section 3.2.1 that fitting an unknown declination to the data would be trivial, given knowledge of the other values.

In addition to finding declination and such, the fringe pattern can be used to calculate the angular diameter of an extended source, which can apply to a lot more than just the Sun if the array has a good enough angular resolution.

The research group found this experiment successful. The baselines were determined with good accuracy and an agreeable value for the Sun's angular diameter was settled upon. The Hail Sagan Research Group looks forward to their next adventure in interferometry and the group members are eager to learn about and gain experience with multiple baseline arrays.

6. References

1. Information on radio antennas, interferometers, and angular resolution
   - Essential Radio Astronomy Online Course[21]
2. Green Bank Observatory information
   - Abstract of paper by Boothroyd, Arnold I.[22]
3. Arecibo Observatory information and more detail on interferometers in general and angular resolution
   - Cornell University website[23]

[21] http://www.cv.nrao.edu/ sransom/web/Ch3.html
[22] http://arxiv.org/abs/1110.1765
[23] http://egg.astro.cornell.edu/alfalfa/ugrad/alfares.htm